Chapter 2
Local Diffusion

2.1 Introduction

Trapped particles exhibit three periodic motions (see Sect. 1.3.1), and consequently possess three adiabatic invariants. Radiation belt electrons can cyclotron resonate with some magnetospheric plasma waves (violating the first and second adiabatic invariants), and then experience the significant acceleration or loss process (Horne and Thorne 1998, 2003; Summers et al. 1998; Roth et al. 1999; Summers and Ma 2000; Albert 2002, 2003, 2004, 2005; Horne et al. 2003a, b, 2005; O'Brien et al. 2003; Albert and Young 2005; Li et al. 2005; Varotsou et al. 2005, 2008; Shprits et al. 2006, 2009b; Xiao and He 2006; Xiao et al. 2007a, b, 2009, 2010a, b; Li et al. 2007; Su and Zheng 2008, 2009; Zheng et al. 2008; Albert and Bortnik 2009; Albert et al. 2009; Su et al. 2009a, c, 2010a, c, 2011a, b, c; Thorne 2010). Such cyclotron resonance driven by various waves is widely believed to control the radiation belt electron dynamics.

The whistler-mode chorus waves are usually distributed in the low-density plasmatrough region approximately from midnight through dawn to noon with frequencies $0.05-0.8\,|\Omega_e|$ ($|\Omega_e|$ is the equatorial electron gyro-frequency) (Tsurutani and Smith 1974, 1977; Koons and Roeder 1990; Meredith et al. 2001; Santolík et al. 2003, 2004). Typical chorus amplitudes are found to be 1–100 pT (Burtis and Helliwell 1975; Meredith et al. 2001, 2003), and even approach 1–3 nT during geomagnetically active periods (Parrot and Gaye 1994; Cattell et al. 2008; Cully et al. 2008). The chorus waves are widely considered to cause the significant acceleration of radiation belt electrons on a timescale of days (e.g., Horne and Thorne 1998; Summers et al. 1998; Horne and Thorne 2003).

The whistler-mode hiss waves mainly occur in the high-density plasmasphere and plasmaspheric plume (Russell et al. 1969; Thorne et al. 1973; Li et al. 2007; Bortnik et al. 2008b, 2009). Their frequencies range from ~100 Hz to several kHz, with amplitudes 10 pT during the quiet times and ~100 pT during the storm times (Smith et al. 1974; Meredith et al. 2004; Summers et al. 2008). The hiss waves can

© Springer-Verlag Berlin Heidelberg 2015

Z. Su, *A Global Kinetic Model for Electron Radiation Belt Formation and Evolution*, Springer Theses, DOI 10.1007/978-3-662-46651-3_2

scatter the energetic electrons into the loss cone and result in their slow decay on a timescale of several days (Lyons and Thorne 1973; Meredith et al. 2007; Su et al. 2010a, 2011a, b, c).

The electromagnetic ion cyclotron (EMIC) waves with typical frequencies 0.1–5.0 Hz are observed in the plasmasphere along the duskside plasmapause or plasmaspheric plumes (Fraser et al. 1996). EMIC emissions typically split into three distinct bands below the hydrogen (H^+), helium (He^+), and oxygen (O^+) ion gyrofrequencies in a multi-ion (H^+, He^+, O^+) plasma. The EMIC waves can efficiently cause the precipitation loss of relativistic electrons on a timescale of hours (Summers et al. 2007a, b).

The quasilinear diffusion theory is widely used to describe the electron PSD evolution due to resonance with waves (e.g., Kennel and Engelmann 1966; Schulz and Lanzerotti 1974; Beutier et al. 1995; Bourdarie et al. 1997; Albert and Young 2005; Xiao et al. 2009; Su et al. 2010a, 2011b). The detailed expressions for the relativistic quasilinear diffusion have been given by Albert (2003, 2005), Glauert and Horne (2005), and their corresponding parallel propagation approximation (PPA) and mean value approximation (MVA) have been proposed by Summers (2005) and Albert (2008). In this chapter, we develop a local diffusion model for radiation belt electron evolution due to cyclotron resonance with various plasma waves. Using this numerical model, we examine the effect of chorus, hiss, and EMIC waves on the radiation belt electrons. Furthermore, in view of ignoring of cross-pitch-angle-momentum diffusion in the previous models, we here evaluate the importance of cross term in the simulations.

2.2 Local Radiation Belt Diffusion Model

2.2.1 Background Magnetic Field

Similar to previous works (e.g., Albert 2003, 2005, 2008; Horne et al. 2003a, 2005; Glauert and Horne 2005; Summers 2005), a typical dipole magnetic field model is used to describe the inner magnetospheric field configuration. It should be mentioned that, during geomagnetic storms, the diffusion coefficients in the different geomagnetic field models may have quantitative differences (Orlova and Shprits 2010).

2.2.2 Basic Equation

The Jacobian matrix between the action space (J_1, J_2, J_3) and observable space (α_e, p, L) can be written as

$$\begin{aligned}\Im &\propto \begin{vmatrix} \partial\mu/\partial\alpha_e & \partial\mu/\partial p & \partial\mu/\partial L \\ \partial J/\partial\alpha_e & \partial J/\partial p & \partial J/\partial L \\ 0 & 0 & \mathrm{d}\Phi/\mathrm{d}L \end{vmatrix} \\ &\propto \frac{\mathrm{d}\Phi}{\mathrm{d}L}\left(\frac{\partial\mu}{\partial\alpha_e}\frac{\partial J}{\partial p} - \frac{\partial\mu}{\partial p}\frac{\partial J}{\partial\alpha_e}\right) \\ &\propto Lp^2\sin\alpha_e\cos\alpha_e\left(I - \frac{\sin\alpha_e}{\cos\alpha_e}\frac{\partial I}{\partial\alpha_e}\right).\end{aligned} \tag{2.1}$$

From Eq. (1.17), we can obtain

$$\frac{\partial I}{\partial\alpha_e} = -\int_{s'_m}^{s_m}\sin\alpha\frac{\partial\alpha}{\partial\alpha_e}\mathrm{d}s + \cos\alpha(s_m)\frac{\partial s_m}{\partial\alpha_e} - \cos\alpha(s'_m)\frac{\partial s'_m}{\partial\alpha_e}. \tag{2.2}$$

Because of $\alpha(s_m) = \alpha(s'_m) = 90°$, the equation above is simplified as

$$\frac{\partial I}{\partial\alpha_e} = -\int_{s'_m}^{s_m}\sin\alpha\frac{\partial\alpha}{\partial\alpha_e}\mathrm{d}s. \tag{2.3}$$

Considering the conservation of first adiabatic invariant in the course of bounce motion

$$\frac{\sin^2\alpha}{B} = \frac{\sin^2\alpha_e}{B_e}, \tag{2.4}$$

we can derive

$$\frac{\partial\alpha}{\partial\alpha_e} = \frac{\tan\alpha}{\tan\alpha_e}. \tag{2.5}$$

Substitution of (2.5) into (2.3) yields

$$I - \frac{\sin\alpha_e}{\cos\alpha_e}\frac{\partial I}{\partial\alpha_e} = \int_{s'_m}^{s_m}\cos\alpha\mathrm{d}s + \int_{s'_m}^{s_m}\frac{\sin^2\alpha}{\cos\alpha}\mathrm{d}s = \int_{s'_m}^{s_m}\frac{1}{\cos\alpha}\mathrm{d}s. \tag{2.6}$$

We further substitute (2.6), (1.12) and (1.14) into (2.1), and obtain the simplified Jacobian matrix

$$\Im \propto L^2 G, \tag{2.7}$$

$$G = p^2 T(\alpha_e)\sin\alpha_e\cos\alpha_e. \tag{2.8}$$

The cyclotron resonance between radiation belt electrons and various plasma waves is a "local" physical process violating the first and second adiabatic invariants (Schulz and Lanzerotti 1974; Shprits et al. 2008a, b). Substitution of the Jacobian matrix (2.7) into (1.35) yields the quasilinear diffusion equation for electron PSD evolution (Schulz and Lanzerotti 1974; Lyons and Williams 1984; Kozyra et al. 1994)

$$\begin{aligned}\frac{\partial f}{\partial t} = &\frac{1}{Gp}\frac{\partial}{\partial \alpha_e}\left[G\left(\langle D_{\alpha\alpha}\rangle\frac{1}{p}\frac{\partial f}{\partial \alpha_e} + \langle D_{\alpha p}\rangle\frac{\partial f}{\partial p}\right)\right] \\ &+ \frac{1}{G}\frac{\partial}{\partial p}\left[G\left(\langle D_{p\alpha}\rangle\frac{1}{p}\frac{\partial f}{\partial \alpha_e} + \langle D_{pp}\rangle\frac{\partial f}{\partial p}\right)\right]\end{aligned} \tag{2.9}$$

with the bounce-averaged pitch-angle, momentum, and cross diffusion coefficients (Lyons and Williams 1984; Glauert and Horne 2005)

$$\langle D_{\alpha\alpha}\rangle = \frac{p^2}{2}\left\langle\frac{(\Delta\alpha_e)^2}{\Delta t}\right\rangle, \tag{2.10}$$

$$\langle D_{\alpha p}\rangle = \frac{p}{2}\left\langle\frac{\Delta\alpha_e \Delta p}{\Delta t}\right\rangle, \tag{2.11}$$

$$\langle D_{pp}\rangle = \frac{1}{2}\left\langle\frac{(\Delta p)^2}{\Delta t}\right\rangle. \tag{2.12}$$

2.2.3 Diffusion Coefficients

The bounce-averaged diffusion coefficients $\langle D_{\alpha\alpha}\rangle$, $\langle D_{pp}\rangle$ and $\langle D_{\alpha p}\rangle = \langle D_{p\alpha}\rangle$ can be obtained through integration of local diffusion coefficients $D_{\alpha\alpha}$, D_{pp} and $D_{\alpha p} = D_{p\alpha}$ along the geomagnetic field line. In the dipole magnetic field, their expressions can be written as (Lyons and Williams 1984)

$$\langle D_{\alpha\alpha}\rangle = \frac{1}{T}\int_0^{\lambda_m} D_{\alpha\alpha}\frac{\cos\alpha}{\cos^2\alpha_e}\cos^7\lambda d\lambda, \tag{2.13}$$

$$\langle D_{pp}\rangle = \frac{1}{T}\int_0^{\lambda_m} D_{pp}\frac{(1+3\sin^2\lambda)^{1/2}}{\cos\alpha}\cos\lambda d\lambda, \tag{2.14}$$

$$\langle D_{\alpha p}\rangle = \langle D_{p\alpha}\rangle = \frac{1}{T}\int_0^{\lambda_m} D_{\alpha p}\frac{(1+3\sin^2\lambda)^{1/4}}{\cos\alpha_e}\cos^4\lambda d\lambda, \tag{2.15}$$

with the latitude λ and the mirror latitude λ_m corresponding to the equatorial pitch-angle α_e. Based on the conservation of first adiabatic invariant and the expression of dipole magnetic field, we can obtain the relation between α_e and λ_m

$$\frac{1}{\sin^2\alpha_e} = \frac{\sin^2\alpha(\lambda_m)}{\sin^2\alpha_e} = \frac{B(\lambda_m)}{B_e} = \frac{(1+3\sin^2\lambda_m)^{1/2}}{\cos^6\lambda_m}, \tag{2.16}$$

$$\cos^{12}\lambda_m + 3\cos^2\lambda_m \sin^4\alpha_e - 4\sin^4\alpha_e = 0. \tag{2.17}$$

The calculation of local diffusion coefficients is implemented through three steps:

1. Determination of wave spectral distribution. The wave frequency ω is usually assumed to obey the typical Gaussian distribution (e.g., Albert 2003, 2005; Summers 2005; Glauert and Horne 2005)

$$B_\omega^2 = \begin{cases} A^2 \exp[-(\omega-\omega_m)^2/(\delta\omega)^2], & \omega_1 \le \omega \le \omega_2 \\ 0, & \text{other} \end{cases}, \tag{2.18}$$

$$A^2 = \frac{2B_t^2}{\pi^{1/2}\delta\omega}\left[\text{erf}\left(\frac{\omega_2-\omega_m}{\delta\omega}\right) + \text{erf}\left(\frac{\omega_m-\omega_1}{\delta\omega}\right)\right]^{-1}, \tag{2.19}$$

with the lower limit ω_1, upper limit ω_2, center ω_m, half-width $\delta\omega$, and amplitude B_t. The tangent X of wave normal angle θ is also assumed to obey the typical Gaussian distribution (e.g., Albert 2003, 2005; Summers 2005; Glauert and Horne 2005)

$$g(X) = \begin{cases} \exp[-(X-X_m)^2/X_\omega^2], & X_1 \le X \le X_2 \\ 0, & \text{other} \end{cases}, \tag{2.20}$$

with the lower limit X_1, upper limit X_2, center X_m and half-width X_ω. When $X_m = X_\omega = 0$, the waves propagate fully parallel along the magnetic field lines.

2. Calculation of resonance roots. The resonance frequency ω and wave vector k satisfy the dispersion relation (Stix 1992) and the n-order cyclotron resonance condition

$$\omega - v_\parallel k_\parallel = -n|\Omega_e|/\gamma, \tag{2.21}$$

where $v_\parallel = v\cos\alpha$ and $k_\parallel = k\cos\theta$ represent the parallel component of electron velocity and wave vector with respect to the background magnetic field. Under high-density approximation (i.e., the ratio of electron plasma frequency ω_{pe} to electron gyrofrequency $|\Omega_e|$ is much larger than 1), the dispersion relation of whistler-mode chorus wave in the electron-proton plasma can be simplified as (Lyons 1974c)

$$V^2 = \left(\frac{ck}{\omega}\right)^2 = \frac{\omega_{pe}^2}{|\Omega_e|^2}\frac{1+M}{M}\Psi^{-1}, \tag{2.22}$$

$$\Psi = 1 - \frac{\omega^2}{\Omega_p|\Omega_e|} - \frac{\sin^2\theta}{2} + \left[\frac{\sin^4\theta}{4} + \frac{\omega^2}{\Omega_p^2}(1-M)^2\cos^2\theta\right]^{1/2}, \tag{2.23}$$

with the ratio of electron and proton masses $M = m_e/m_p = 1/1836$ and the proton gyrofrequency Ω_p. In a multi-component plasma (e^-, H^+, He^+, O^+), the dispersion relation of parallel-propagation EMIC waves is (Summers and Thorne 2003)

$$\frac{c^2k^2}{\omega^2} = 1 - \frac{\omega_{pe}^2}{\omega(\omega + |\Omega_e|)} - \sum_{j=1}^{3} \frac{\omega_{pj}^2}{\omega(\omega - \Omega_j)}, \tag{2.24}$$

where $\Omega_j|_{j=1,2,3}$ represent the gyro-frequencies of H^+, He^+ and O^+, and ω_{pj} denote the jth ion plasma frequency.

3. Expression of diffusion coefficients. The quasilinear description of cyclotron resonance was first proposed by Kennel and Engelmann (1966). Based on the works of Kennel and Engelmann (1966), Lyons (1974a, b, c), Lyons and Williams (1984), Albert (2003, 2005), Glauert and Horne (2005) have given the expression of relativistic diffusion coefficients for the obliquely propagating plasma waves

$$\begin{pmatrix} D_{\alpha\alpha} & D_{\alpha p} \\ D_{p\alpha} & D_{pp} \end{pmatrix} = \begin{pmatrix} \tilde{D}_{\alpha\alpha} & \tilde{D}_{\alpha p} \\ \tilde{D}_{p\alpha} & \tilde{D}_{pp} \end{pmatrix} |\Omega_e|^2 \frac{B_\omega^2}{B^2} \frac{p^2}{\gamma^2}, \tag{2.25}$$

$$\begin{pmatrix} \tilde{D}_{\alpha\alpha} & \tilde{D}_{\alpha p} \\ \tilde{D}_{p\alpha} & \tilde{D}_{pp} \end{pmatrix} = \sum_{n=n_1}^{n_2} \int_{X_1}^{X_2} X \mathrm{d}X \begin{pmatrix} \tilde{D}_{\alpha\alpha}^{nX} & \tilde{D}_{\alpha p}^{nX} \\ \tilde{D}_{p\alpha}^{nX} & \tilde{D}_{pp}^{nX} \end{pmatrix}, \tag{2.26}$$

$$\tilde{D}_{\alpha\alpha}^{nX} = \sum_i \frac{\omega^2(\sin^2\alpha + n|\Omega_e|/\gamma\omega)^2}{4\pi v_\parallel^2(1+X^2)N(\omega)} \frac{g(X)|\Phi_{n,\mathbf{k}}|^2}{\left|v_\parallel - \partial\omega/\partial k_\parallel\big|_X\right|}\Bigg|_{\substack{\omega=\omega_i \\ k=k_i}}, \tag{2.27}$$

$$N(\omega) = \frac{1}{2\pi^2} \int_0^\infty g(X) \left| J\left(\frac{k_\perp, k_\parallel}{\omega, X}\right) \right| k_\perp \mathrm{d}X, \tag{2.28}$$

$$J\left(\frac{k_\perp, k_\parallel}{\omega, X}\right) = -k_\parallel \frac{\partial k_\parallel}{\partial\omega}\bigg|_X = -k\cos^2\theta \frac{\partial k}{\partial\omega}\bigg|_X, \tag{2.29}$$

$$\begin{aligned} |\Phi_{n,\mathbf{k}}|^2 &= \left[\left(\frac{2D}{V^2 - S}\right)^2 + \left(\frac{2P\cos\theta}{V^2\sin^2\theta - P}\right)^2\right]^{-1} \\ &\times \left[\left(\frac{V^2 - L}{V^2 - S}\right) J_{n+1} + \left(\frac{V^2 - R}{V^2 - S}\right) J_{n-1} + \frac{V^2\cot\alpha\sin 2\theta}{V^2\sin^2\theta - P} J_n\right]^2, \end{aligned} \tag{2.30}$$

$$R = \frac{\omega_{pe}^2}{|\Omega_e|^2} \frac{|\Omega_e|}{\omega} \left[\frac{1+M}{1 - M - (\omega/|\Omega_e| - \Omega_p/\omega)}\right], \tag{2.31}$$

$$L = -\frac{\omega_{pe}^2}{|\Omega_e|^2}\frac{|\Omega_e|}{\omega}\left[\frac{1+M}{1-M+(\omega/|\Omega_e|-\Omega_p/\omega)}\right], \tag{2.32}$$

$$P = -\frac{\omega_{pe}^2}{|\Omega_e|^2}\frac{|\Omega_e|^2}{\omega^2}(1+M), \tag{2.33}$$

$$S = \frac{R+L}{2}, \tag{2.34}$$

$$D = \frac{R-L}{2}, \tag{2.35}$$

$$\tilde{D}_{\alpha p}^{nX} = \tilde{D}_{p\alpha}^{nX} = \tilde{D}_{\alpha\alpha}^{nX}\left[\frac{\sin\alpha\cos\alpha}{-\sin^2\alpha - n|\Omega_e|/\gamma\omega}\right]\Bigg|_{\substack{\omega=\omega_i\\k=k_i}}, \tag{2.36}$$

$$\tilde{D}_{pp}^{nX} = \tilde{D}_{\alpha\alpha}^{nX}\left[\frac{\sin\alpha\cos\alpha}{-\sin^2\alpha - n|\Omega_e|/\gamma\omega}\right]^2\Bigg|_{\substack{\omega=\omega_i\\k=k_i}}. \tag{2.37}$$

Here n_1 and n_2 are the upper and lower limits of resonance orders; ω_i and k_i are the i-th resonant frequency and wave number, the subscripts $\perp$ and $\parallel$ represent the parallel and perpendicular components with respect to the background magnetic field; the argument of n-order Bessel function is $-k_\perp p_\perp/(m_e|\Omega_e|)$. Based on the work of Kennel and Engelmann (1966), Summers (2005) and Tao et al. (2011a) had presented the expressions of relativistic diffusion coefficients for the parallel propagation plasma waves

$$D_{\alpha\alpha} = |\Omega_e|^2\left(\frac{p^2}{\gamma^2}I_0 - 2\cos\alpha\frac{m_e c p}{\gamma}I_1 + \cos^2\alpha m_e^2 c^2 I_2\right), \tag{2.38}$$

$$D_{pp} = m_e^2 c^2 |\Omega_e|^2 \sin^2\alpha I_2, \tag{2.39}$$

$$D_{\alpha p} = D_{p\alpha} = -m_e c p |\Omega_e|^2 \sin\alpha\left(\frac{I_1}{\gamma} - \frac{m_e c\cos\alpha}{p}I_2\right), \tag{2.40}$$

$$I_s = \frac{\pi}{4}\sum_i\left[\frac{B_\omega^2}{B^2}\left(\frac{\omega}{ck}\right)^s\left|1-\cos\alpha\frac{p}{\gamma m_e}\frac{\mathrm{d}k}{\mathrm{d}\omega}\right|^{-1}\right]\Bigg|_{\substack{\omega=\omega_i\\k=k_i}}, \quad s=0,1,2. \tag{2.41}$$

2.2.4 Numerical Method

The quasilinear diffusion equation includes three parts: pitch-angle diffusion, momentum diffusion, and cross diffusion. Utilizing the standard finite difference methods to this equation often leads to the numerical instability associated with the cross

diffusion (Albert 2004; Albert and Young 2005). Albert and Young (2005) proposed a variable transformation method to diagonalize the diffusion matrix. In this special variable space, cross diffusion is removed and the typical implicit method can be directly used to solve the equation. Obviously, such transformation depends on the diffusion coefficients, and the different diffusion coefficients would require different transformation variables. Tao et al. (2008, 2009) adopted a Monte Carlo method or a layer method to solve this equation. But these methods are inefficient compared to the direct difference method. We have developed a Hybrid Finite Difference Method (Xiao et al. 2009; Su et al. 2009c, 2011c) to fully solve this quasilinear diffusion Eq. (2.9).

The diffusion Eq. (2.9) is rewritten as

$$\frac{\partial f}{\partial t} = \frac{1}{Gp}\frac{\partial}{\partial \alpha_e}\left(\frac{G\langle D_{\alpha\alpha}\rangle}{p}\frac{\partial f}{\partial \alpha_e}\right) + \frac{1}{Gp}\frac{\partial}{\partial \xi}\left(\frac{G\langle D_{pp}\rangle}{p}\frac{\partial f}{\partial \xi}\right) + \frac{1}{Gp}\frac{\partial}{\partial \alpha_e}\left(\frac{G\langle D_{\alpha p}\rangle}{p}\right)\frac{\partial f}{\partial \xi} + \frac{1}{Gp}\frac{\partial}{\partial \xi}\left(\frac{G\langle D_{\alpha p}\rangle}{p}\right)\frac{\partial f}{\partial \alpha_e} + \frac{2\langle D_{\alpha p}\rangle}{p^2}\frac{\partial^2 f}{\partial \alpha_e \partial \xi}, \tag{2.42}$$

with the variable ξ defined as $\xi = \ln\dfrac{p}{m_e c}$. Based on the split-operator technique (Strang 1968; Kim et al. 1999), the equation above is split into

$$\frac{\partial f}{\partial t} = \frac{1}{Gp}\frac{\partial}{\partial \alpha_e}\left(\frac{G\langle D_{\alpha\alpha}\rangle}{p}\frac{\partial f}{\partial \alpha_e}\right), \tag{2.43}$$

$$\frac{\partial f}{\partial t} = \frac{1}{Gp}\frac{\partial}{\partial \xi}\left(\frac{G\langle D_{pp}\rangle}{p}\frac{\partial f}{\partial \xi}\right), \tag{2.44}$$

$$\frac{\partial f}{\partial t} = \frac{1}{Gp}\frac{\partial}{\partial \xi}\left(\frac{G\langle D_{\alpha p}\rangle}{p}\right)\frac{\partial f}{\partial \alpha_e} + \frac{1}{Gp}\frac{\partial}{\partial \alpha_e}\left(\frac{G\langle D_{\alpha p}\rangle}{p}\right)\frac{\partial f}{\partial \xi} + \frac{2\langle D_{\alpha p}\rangle}{p^2}\frac{\partial^2 f}{\partial \alpha_e \partial \xi}. \tag{2.45}$$

At each time-step, the solving of Eq. (2.42) can be implemented by the successive solving of Eqs. (2.43−2.45). The diagonal Eqs. (2.43) and (2.44) are solved by the fully-implicit method, while the off-diagonal Eq. (2.45) is solved by the alternative direction implicit (ADI) method (Strang 1968). The whole numerical algorithm is named as the Hybrid Finite Difference Method (HFD) due to the combination of two different finite difference methods. In the quasilinear dynamic simulations of radiation belt, ring current and aurora, this HFD method has been widely used by our group (Su et al. 2009a, b, c, 2010a, b, c, 2011a, b, c; Xiao et al. 2009, 2010a, b, 2011) and other researchers (Fok et al. 2010; Thorne et al. 2010; Tao et al. 2011b; Zheng et al. 2011).

2.3 Idealized Simulations

Because of the numerical difficulty associated with cross diffusion, the previous work often ignore the cross diffusion terms (e.g., Varotsou et al. 2005, 2008; Li et al. 2007). In this section, we calculate the diffusion coefficients of chorus, hiss, and EMIC waves, and then fully solve the diffusion equation to quantify the effect of various waves on radiation belt electrons. In addition, through comparison between simulations with and without cross terms, we attempt to evaluate the importance of cross diffusion.

We concentrate on the local acceleration and loss processes in the center ($L = 4.5$) of the outer radiation belt. The computational range covers $\alpha_e \in [0°, 90°]$ and $E_k \in [0.2\,\text{MeV}, 10.0\,\text{MeV}]$. The uniform grids are adopted in the (α_e, ξ) space with grid numbers 91×81. The time-step is set to be $\Delta t = 1$ s. It should be noted that only the electron fluxes in the energy range $E_k \in [0.2\,\text{MeV}, 5.0\,\text{MeV}]$ are plotted to clearly identify the ~MeV electron evolution.

The initial electron PSD is assumed to obey the Kappa-type distribuion (Vasyliunas 1968; Maksimovic et al. 1997a, b; Viñas et al. 2005; Xiao 2006; Xiao et al. 2008a, b, c)

$$f(t = 0, \alpha_e, p) = C \left(\frac{p \sin \alpha_e}{\theta_\kappa} \right)^{2l} \left[1 + \frac{p^2}{\kappa \theta_\kappa^2} \right]^{-(\kappa + l + 1)}, \tag{2.46}$$

$$C = \frac{N \Gamma(\kappa + l + 1)}{\pi^{3/2} \theta_\kappa^{3/2} \kappa^{(l+3/2)} \Gamma(l + 1) \Gamma(\kappa - 1/2)}, \tag{2.47}$$

with the loss cone prameter l, effective thermal parameter θ_κ^2 electron density N, spectral index κ, and Gamma function Γ. Here these parameters are empirically chosen to be $\theta_\kappa^2 = 0.15$, $l = 0.5$ and $\kappa = 6$ (Xiao et al. 2009).

At the loss cone boundary $\alpha_e = \alpha_L$, the electron PSD is set to be zero. At $\alpha_e = 90°$, the equivalent extrapolation boundary condition is adopted. At the upper and lower energy boundaries, the electron PSDs are fixed.

2.3.1 Chorus

Based on the previous works (Meredith et al. 2001, 2002, 2003; Horne et al. 2005; Li et al. 2007), we choose different parameters for nightside and dayside chorus waves and the corresponding background plasma. We assume the constant electron density along the geomagnetic file lines. The equatorial ratio between electron plasma frequency ω_{pe} and gyrofrequency $|\Omega_e|$ is set to be 3.8 in the nightside and 4.6 in the dayside. At the nightside, the chorus waves are distributed over the latitudinal region $|\lambda| < 15°$ with the spectral parameters $B_t = 50$ pT, $\omega_1 = 0.05|\Omega_e|$, $\omega_2 = 0.65|\Omega_e| \delta\omega = 0.15|\Omega_e|$, $\omega_m = 0.35|\Omega_e|$, $X_m = 0$, $X_\omega = 0.577$, $X_1 = 0$ and

$X_2 = 1$. At the dayside, the chorus waves are distributed in the latitudinal region $\lambda \leq 35°$ with the spectral parameters $B_t = 10^{0.75+0.04\lambda}$ pT, $\omega_1 = 0.1|\Omega_e|$, $\omega_2 = 0.3|\Omega_e|$, $\delta\omega = 0.1|\Omega_e|$, $\omega_m = 0.2|\Omega_e|$, $X_m = 0$, $X_\omega = 0.577$, $X_1 = 0$ and $X_2 = 1$. On both sides, the resonance orders $n = 0, \pm 1, \ldots, \pm 5$ are taken into account. It should be noted that these parameters have been frequently used to simulate the chorus-driven radiation belt electron evolution during storms (e.g., Li et al. 2007; Shprits et al. 2009a, b; Subbotin et al. 2010; Su et al. 2009a, 2011a, b, c, 2010a, c; Xiao et al. 2009, 2010b).

Figure 2.1 shows the two-dimensional distribution of diffusion rates for the nightside and dayside chorus waves in the (α_e, E_k) space, and Fig. 2.2 plots the diffusion coefficient profiles at the selected energies. Obviously, the pitch-angle and momentum diffusion rates behave smoothly, but the cross diffusion rates exhibit rapid and significant fluctuations which can easily lead to numerical instability (Albert 2004; Albert and Young 2005). The maximum values of pitch-angle diffusion rates are about 10 times larger than those of momentum diffusion rates, and the maximum values of momentum and cross diffusion rates are generally comparable (implying that the ignoring of cross diffusion rates is unreasonable). The diffusion rates for nightside and dayside chorus waves have quite different distributions. The diffusion rates of nightside chorus waves peak at the large equatorial pitch-angles (near $\alpha_e = 90°$). In contrast, the diffusion rates of dayside chorus waves peak at the small equatorial pitch-angles (near $\alpha_e = \alpha_L$).

The energetic electrons drift around the Earth on closed paths, quasi-periodically passing through the spatial regions with different types of waves. We assume that the nightside and dayside chorus waves are distributed 25 % of drift paths, respectively. The drift-averaged diffusion coefficients are input into Eq. (2.9) to simulate the evolution of electron PSD f and flux $j = p^2 f$. Figures 2.3 and 2.4 present the electron flux evolution with and without cross diffusion. As shown in the simulations with cross diffusion, the chorus waves can effectively accelerate the electrons and enhance significantly the energetic electron fluxes especially at the large equatorial pitch-angles ($\alpha_e > 45°$). Within two days, the equatorially-trapped electron fluxes at energies $E_k = 0.5$, 1.0 and 2.0 MeV can increase by about 3, 30, and 60 times, respectively. The ignoring of cross diffusion can largely overestimate the acceleration effect of chorus waves. After two days, the equatorially-trapped electron fluxes at energies $E_k = 0.5$, 1.0, and 2.0 MeV are overestimated by about 3, 6, and 5 times at the large pitch-angles, and by about 10, 50, and 200 times at the small pitch-angles, respectively. These results suggest that cross diffusion plays an important role in chorus-electron cyclotron resonance.

2.3.2 Hiss

We assume constant electron density along the magnetic field line, and set the equatorial $\omega_{pe}/|\Omega_e| = 15$ (Li et al. 2007). The hiss waves are distributed in the latitudinal region $\lambda < 40°$ with spectral properties $B_t = 0.1$ nT, $\omega_1 = 0.01|\Omega_e|$, $\omega_2 = 0.21|\Omega_e|$,

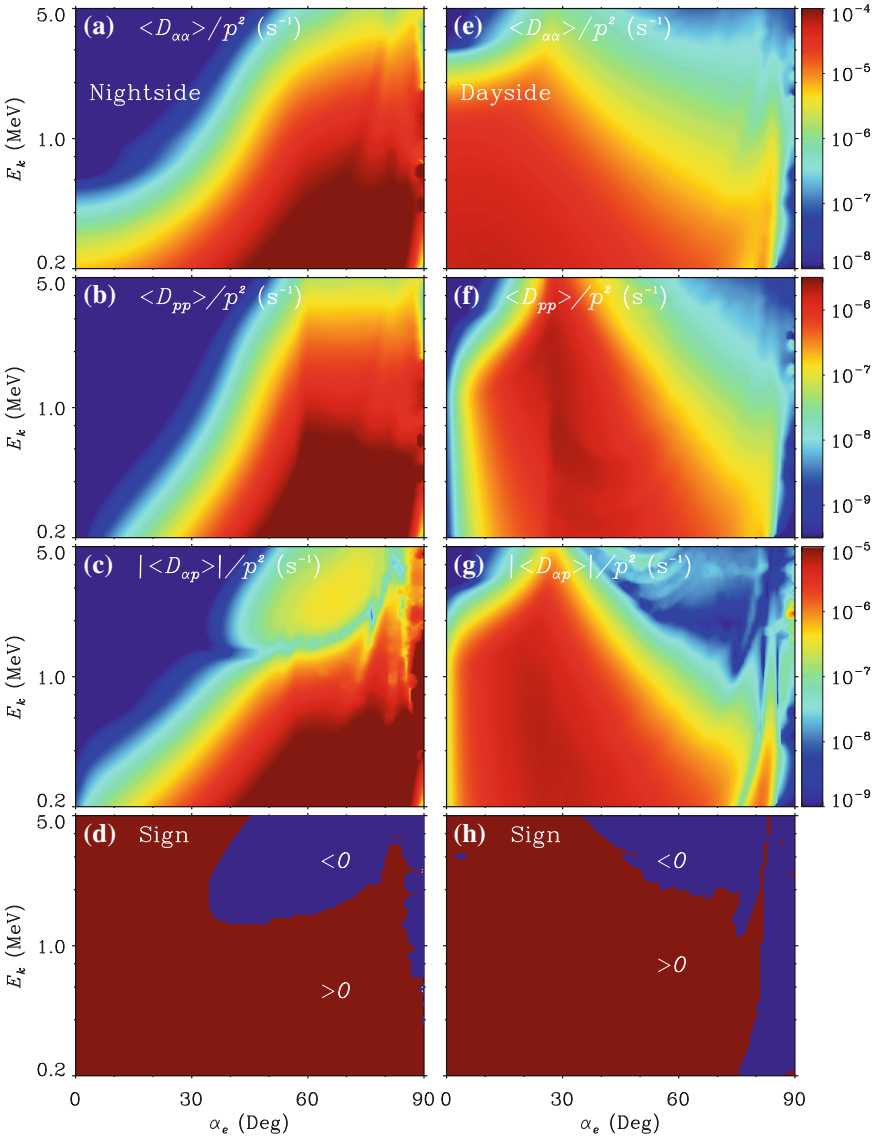


Fig. 2.1 Distribution of nightside (*left*) and dayside (*right*) chorus-driven diffusion rates in the (α_e, E_k) space

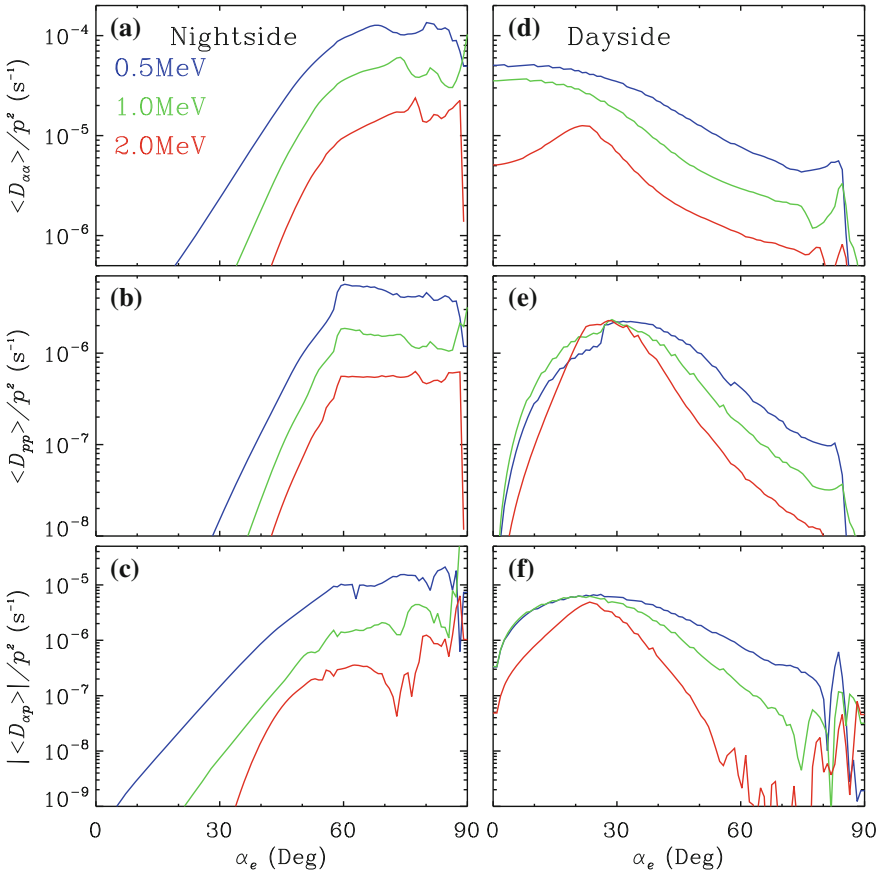


Fig. 2.2 Nightside (*left*) and dayside (*right*) chorus-driven diffusion rate profiles at energies $E_k = 0.5$, 1.0 and 2.0 MeV

$\delta\omega = 0.03|\Omega_e|, \omega_m = 0.06|\Omega_e|, X_m = 0, X_\omega = 0.577, X_1 = 0$ and $X_2 = 1$. Similar to chorus waves, the cyclotron resonance orders $n = 0, \pm 1, \ldots, \pm 5$ are taken into account for hiss waves. These parameters have been frequently adopted to simulate the hiss-driven radiation belt electron evolution (e.g., Li et al. 2007; Shprits et al. 2009b; Xiao et al. 2009; Su et al. 2010a, 2011a, b, c).

The distributions and profiles of obtained hiss-driven diffusion rates are shown in Figs. 2.5 and 2.6. The maximum diffusion rates occur at the large equatorial pitch-angles and small energies. As the energy increases, the diffusion rates decrease gradually. The maximum values of pitch-angle and cross diffusion rates are 3000 and 50 times larger than the momentum diffusion rates, respectively.

We assume that the hiss waves are distributed in the 15 % of electron drift pathes (Li et al. 2007), input the drift-averaged diffusion coefficients into the Eq. (2.9), and obtain the electron flux $j = p^2 f$ evolution (given in Figs. 2.7 and 2.8). As shown

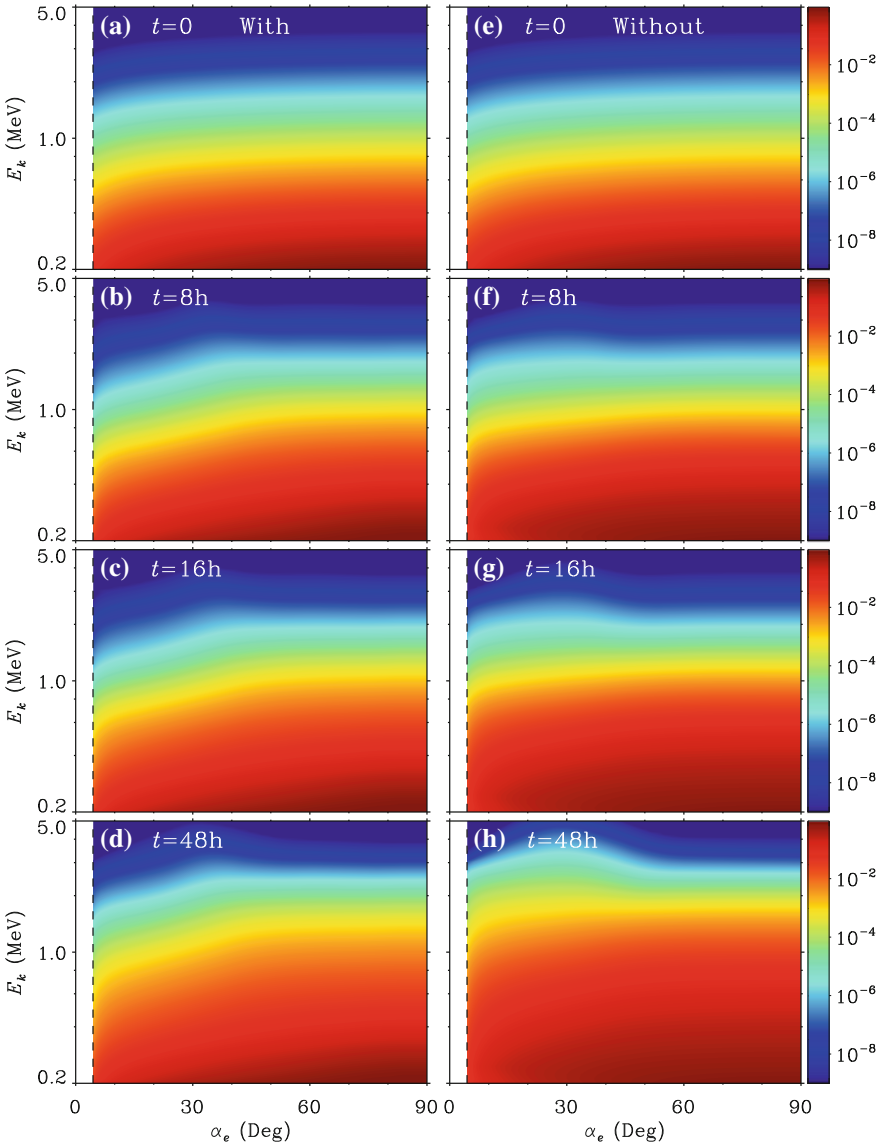


Fig. 2.3 Evolution of chorus-driven electron flux $j = p^2 f$ (arbitrary unit) in the (α_e, E_k) space. The *left* and *right* panels correspond to the simulations with and without cross diffusion

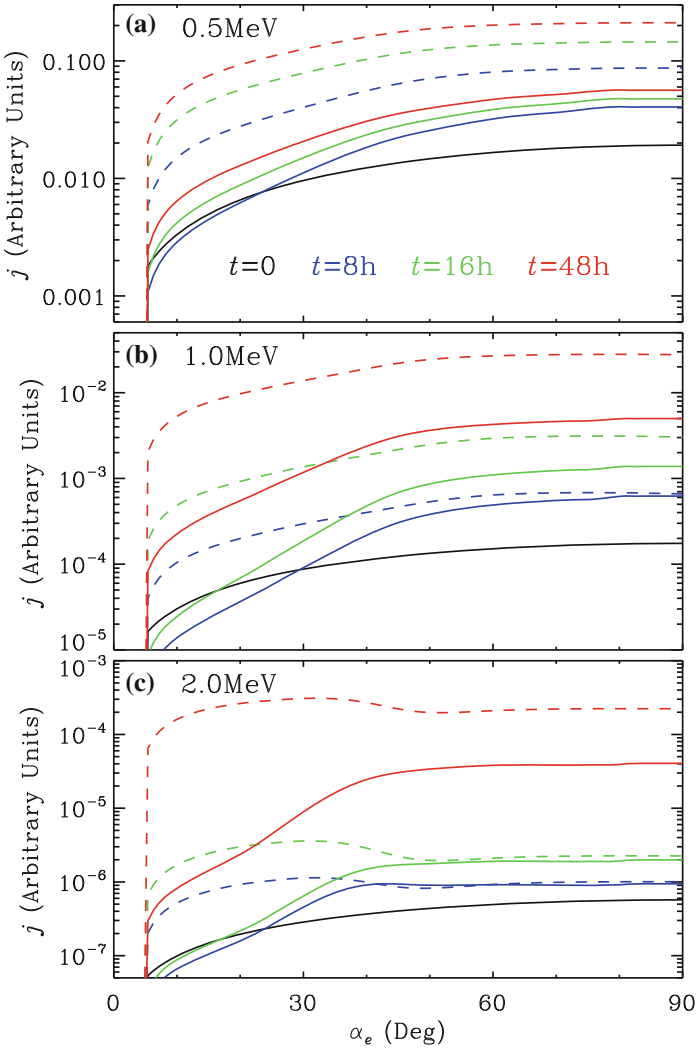


Fig. 2.4 Electron flux profiles $j = p^2 f$ at the selected time points. The *solid* and *dashed lines* represent the simulations with and without cross diffusion

in the simulations with cross diffusion, the hiss waves can effectively scatter the energetic electrons especially at the large pitch-angles, drive them toward the loss cone, and produce the electron precipitation loss. Since the diffusion coefficients generally decrease with increasing energy, the hiss waves show weaker loss effect on the electrons with larger energies. Within two days, the equatorially-trapped electron fluxes at energies $E_k = 0.5, 1.0$, and 2.0 MeV are cut to 1/5, 1/2, and 2/3, respectively.

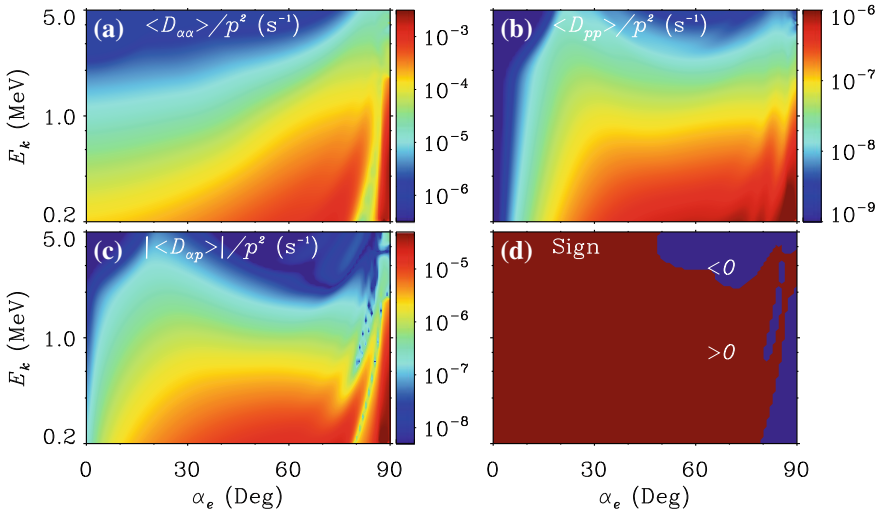


Fig. 2.5 Distribution of hiss-driven diffusion rates in the (α_e, E_k) space

Ignoring of cross diffusion can lead to the overestimate of electron fluxes by <2 times, indicating that cross diffusion plays an insignificant role in hiss-electron cyclotron resonance.

2.3.3 EMIC

The electron density is fixed along the magnetic field line, and the equatorial $\omega_{pe}/|\Omega_e|$ is specified as 15 (Li et al. 2007). It should be mentioned that, the statistical characteristics of EMIC waves are not clear (Shprits et al. 2009a). Based on previous works (Li et al. 2007; Summers et al. 2007b), we concentrate here on the parallel-propagating He^+ band EMIC waves. The background ion composition is assumed to be $70\%H^+ + 20\%He^+ + 10\%O^+$. The EMIC waves are distributed in the low latitude region $\lambda < 15°$ with spectral parameters $B_t = 1.0$ nT, $\omega_1 = 3.45\Omega_{O^+}$, $\omega_2 = 3.95\Omega_{O^+}$, $\delta\omega = 0.25\Omega_{O^+}$ and $\omega_m = 3.70\Omega_{O^+}$. For such parallel-propagating L-mode waves, only the $n = 1$ order cyclotron resonance can occur (Summers 2005).

The obtained diffusion rate distributions and profiles are plotted in Figs. 2.9 and 2.10. The modeled EMIC waves can only resonate with the high energy electrons (Summers 2005; Summers et al. 2007a). The minimum resonant energy for the present EMIC waves is about $E_{kmin} = 0.4$ MeV. As the energy increases, the resonant pitch-angles extend toward $\alpha_e = 90°$. The maximum values of pitch-angle diffusion rates are about 2×10^7 and 4×10^3 times larger than those of momentum and cross diffusion rates, respectively, indicating the dominance of pitch-angle diffusion.

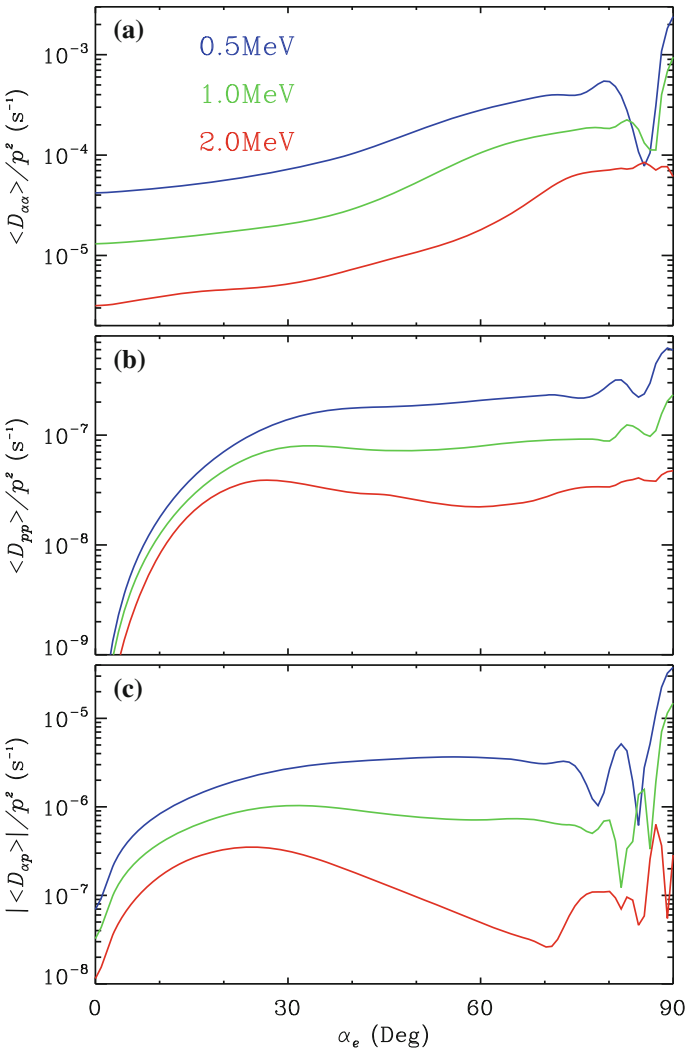


Fig. 2.6 Hiss-driven diffusion rate profiles at energies $E_k = 0.5$, 1.0 and 2.0 MeV

The EMIC waves are assumed to be distributed in the 5 % of drift pathes (Li et al. 2007; Shprits et al. 2009b; Su et al. 2010a, 2011a, b, c), and the obtained electron flux evolution is plotted in Figs. 2.11 and 2.12. Due to the dominance of pitch-angle diffusion, there is no notable difference between the simulation results including and ignoring cross diffusion. The EMIC waves can cause rapid precipitation loss of energetic electrons. After 12 h, the electron fluxes near the loss cone at energies $E_k = 0.5$, 1.0 and 2.0 MeV are cut to 1/50, 1/200, and 1/3000, respectively. The EMIC waves cannot scatter the energetic electron near $\alpha_e = 90°$, but the hiss waves

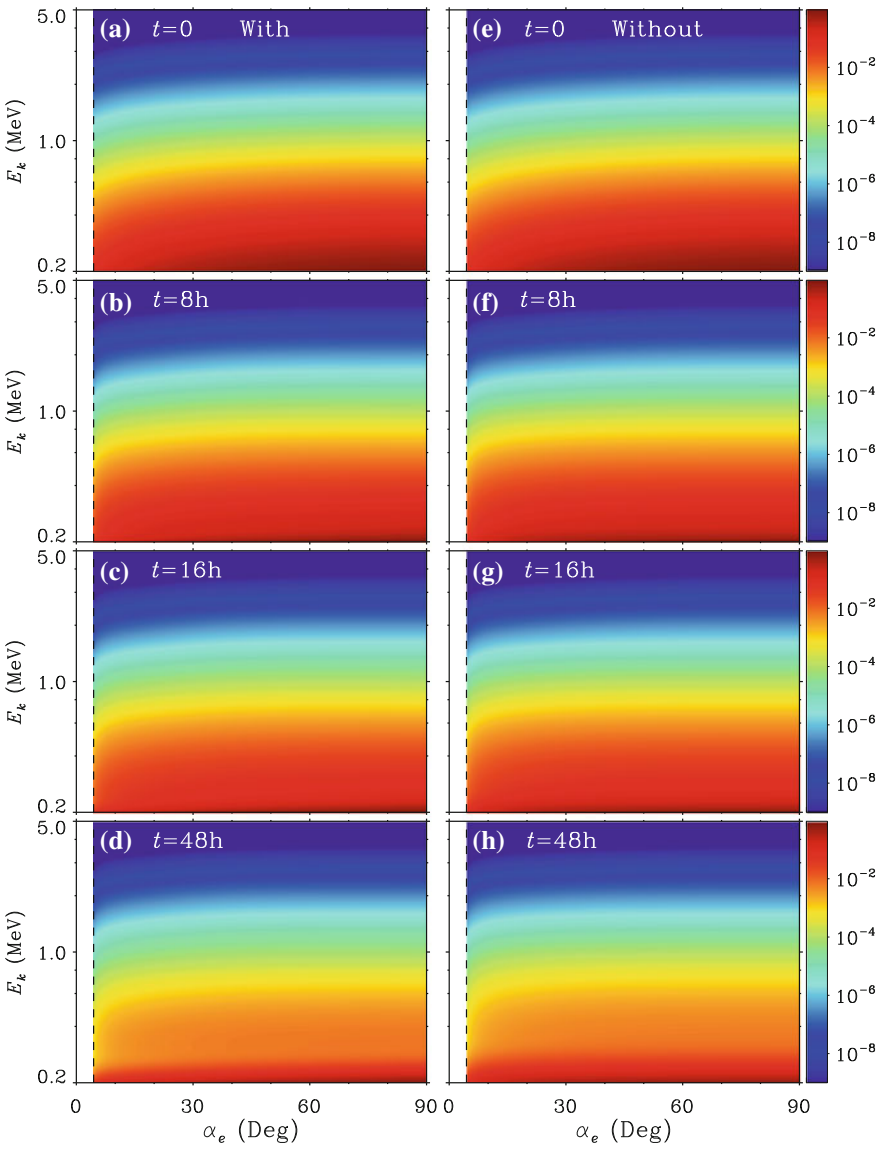


Fig. 2.7 Evolution of chorus-driven electron flux $j = p^2 f$ (arbitrary unit) in the (α_e, E_k) space. The *left* and *right panels* correspond to the simulations with and without cross diffusion

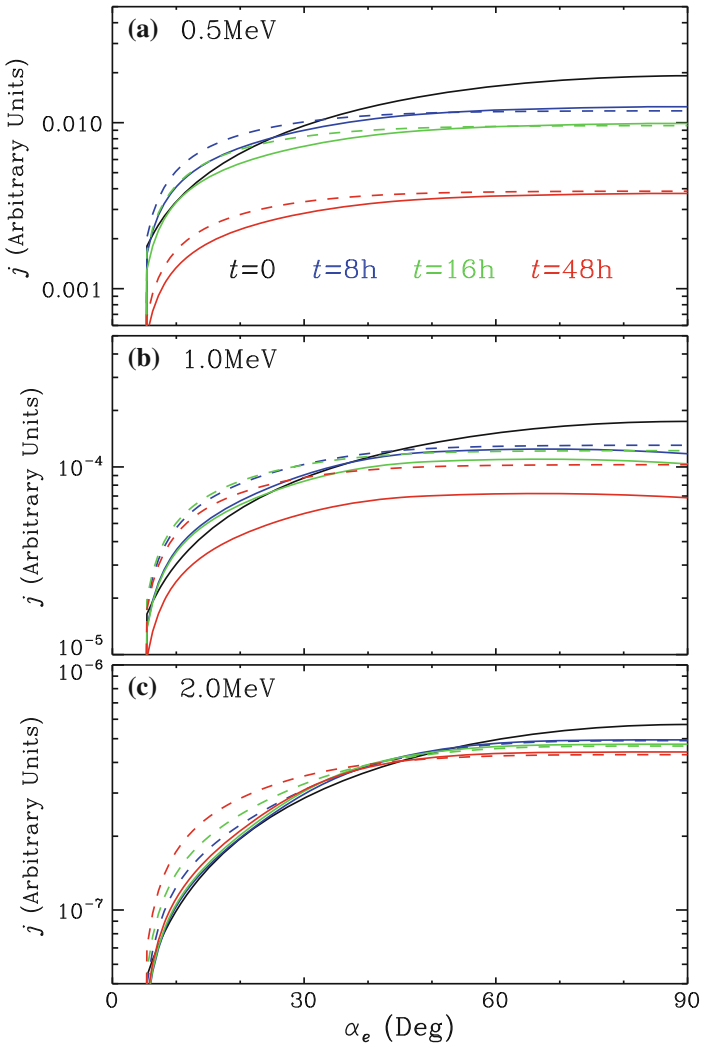


Fig. 2.8 Electron flux profiles $j = p^2 f$ at the selected time points. The *solid* and *dashed lines* represent the simulations with and without cross diffusion

can drive the electrons with the large pitch-angles toward the loss cone. Hence, the combination of hiss and EMIC waves would produce more effective precipitation loss of radiation belt electrons (Li et al. 2007; Su et al. 2011c).

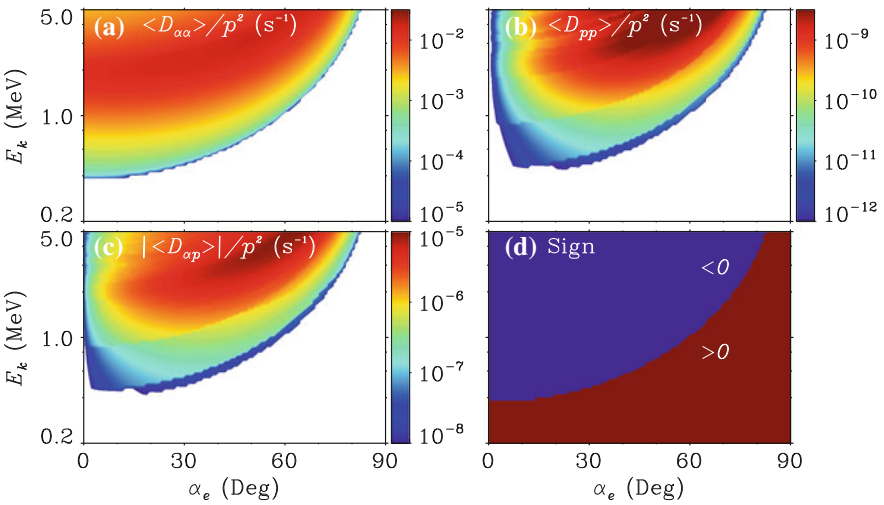


Fig. 2.9 Distribution of EMIC-driven diffusion rates in the (α_e, E_k) space

2.4 Conclusions and Discussions

We have developed an electron radiation belt local diffusion model based on the quasilinear theory. The quasilinear diffusion equation involves the diffusion in pitch-angle, momentum, and cross terms. The including of cross diffusion often yields numerical instability for the common finite difference methods (Albert 2004; Albert and Young 2005). We propose an efficient, stable, and easily-programming numerical scheme, named HFD, to fully solve this diffusion equation (Su et al. 2009c, 2011c; Xiao et al. 2009). This numerical scheme has been widely used by our research group (Su et al. 2009a, b, c, 2010a, b, c, 2011a, b, c; Xiao et al. 2009, 2010b, a, 2011) and other researchers (Fok et al. 2010; Thorne et al. 2010; Tao et al. 2011b; Zheng et al. 2011).

Using this local diffusion model, we have analyzed the effect of chorus, hiss and EMIC on the radiation belt electrons, and particularly identify the importance of cross diffusion.

1. The present simulation results with cross diffusion support the previous finding. The chorus waves can effectively accelerate the energetic electrons, especially at the large pitch-angles: the equatorially trapped energetic electron fluxes can increase by about 1–2 orders of magnitude within 2 days. The hiss waves can drive the electrons at the large pitch-angles toward the loss cone: the equatorially-trapped energetic electron fluxes can be cut to 1/5–2/3 within 2 days. The EMIC waves can effectively scatter the relativistic electrons into the loss cone: the relativistic electron fluxes near the loss cone can be cut to 1/3000–1/50 within 12 h.

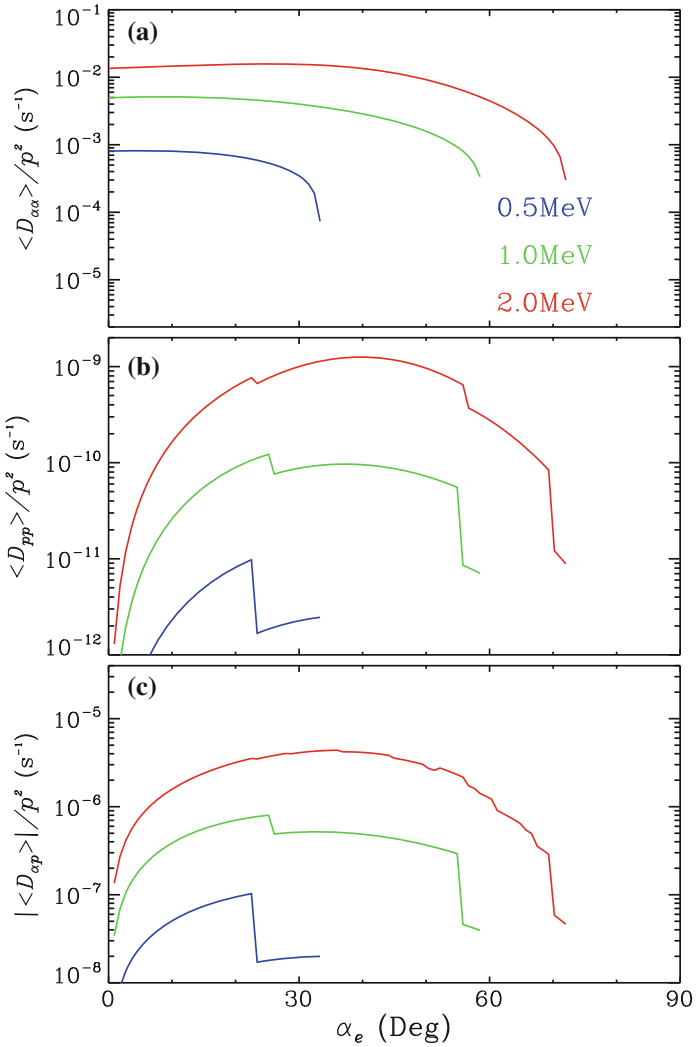


Fig. 2.10 EMIC-driven diffusion rate profiles at energies $E_k = 0.5$, 1.0 and 2.0 MeV

2. Cross diffusion plays different roles in the different wave-particle interactions. Ignoring of cross diffusion can significantly overestimate the electron fluxes for cyclotron resonance with chorus, slightly overestimate the electron fluxes for the cyclotron resonance with hiss, but have no effect on the electron fluxes for cyclotron resonance with EMIC.

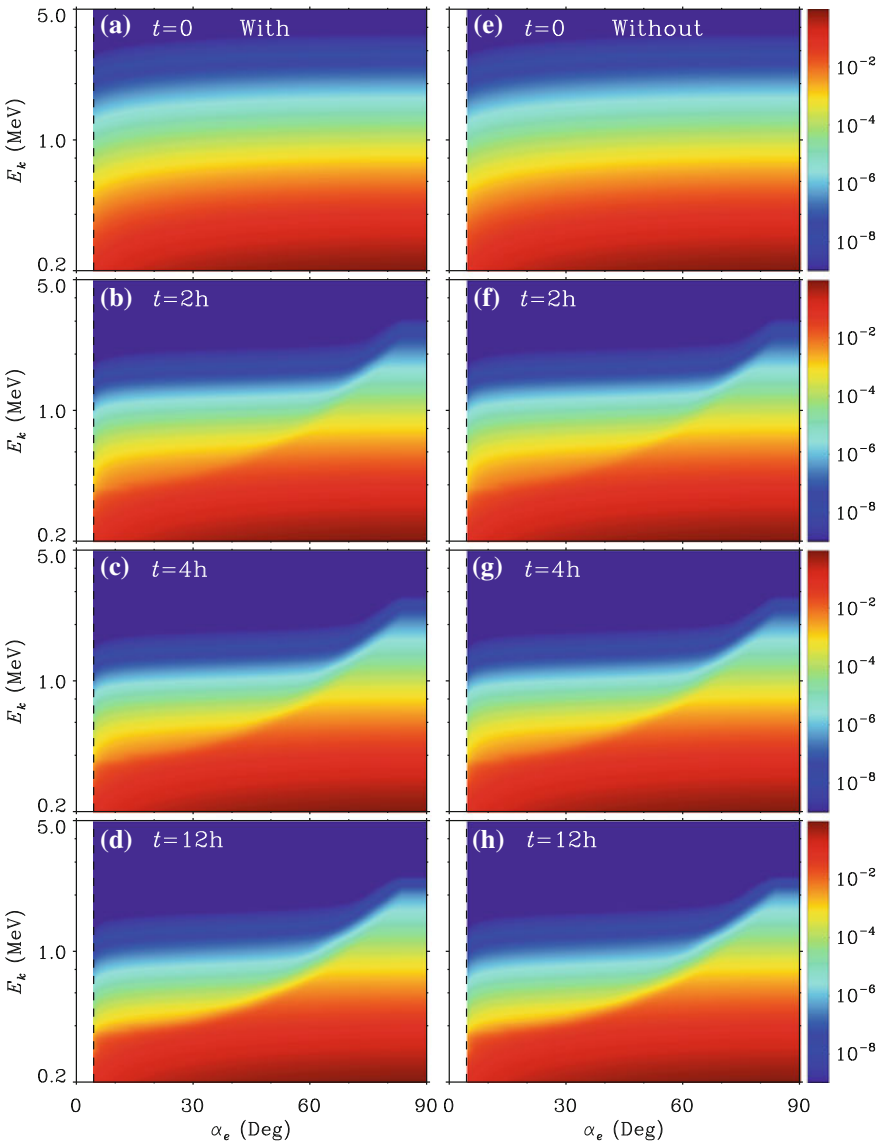


Fig. 2.11 Evolution of EMIC-driven electron flux $j = p^2 f$ (arbitrary unit) in the (α_e, E_k) space. The *left* and *right panels* correspond to the simulations with and without cross diffusion

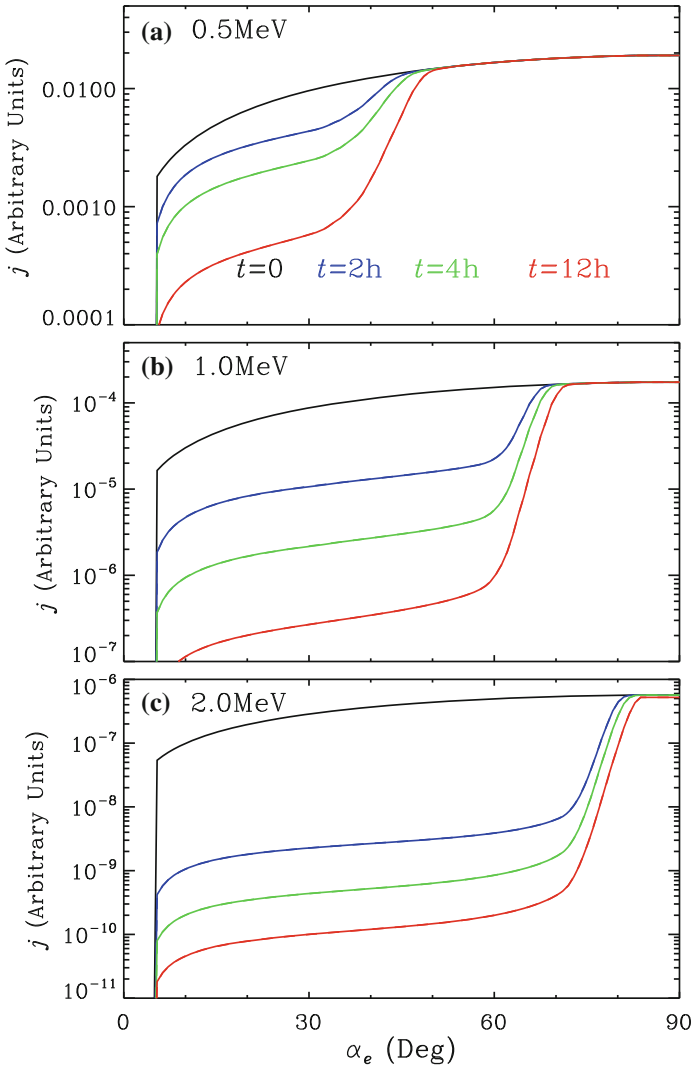


Fig. 2.12 Electron flux profiles $j = p^2 f$ at the selected time points. The *solid* and *dashed lines* represent the simulations with and without cross diffusion, which coincide with each other

References

Albert JM (1999) Analysis of quasi-linear diffusion coefficients. J Geophys Res 104:2429–2442. doi:10.1029/1998JA900113

Albert JM (2002) Nonlinear interaction of outer zone electrons with VLF waves. Geophys Res Lett 29:1275. doi:10.1029/2001GL013941

Albert JM (2003) Evaluation of quasi-linear diffusion coefficients for EMIC waves in a multispecies plasma. J Geophys Res 108(A8):1249. doi:10.1029/2002JA009792

Albert JM (2004) Using quasi-linear diffusion to model acceleration and loss from wave-particle interactions. Space Weather 2:9. doi:10.1029/2004SW000069

Albert JM (2005) Evaluation of quasi-linear diffusion coefficients for whistler mode waves in a plasma with arbitrary density ratio. J Geophys Res 110(A9):A03,218, doi:10.1029/2004JA010844

Albert JM (2008) Efficient approximations of quasi-linear diffusion coefficients in the radiation belts. J Geophys Res 113(A06):208. doi:10.1029/2007JA012936

Albert JM, Bortnik J (2009) Nonlinear interaction of radiation belt electrons with electromagnetic ion cyclotron waves. Geophys Res Lett 36(L12):110. doi:10.1029/2009GL038904

Albert JM, Young SL (2005) Multidimensional quasi-linear diffusion of radiation belt electrons. Geophys Res Lett 32(L14):110. doi:10.1029/2005GL023191

Albert JM, Meredith NP, Horne RB (2009) Three-dimensional diffusion simulation of outer radiation belt electrons during the october 9, 1990, magnetic storm. J Geophys Res 114(A09):214. doi:10.1029/2009JA014336

Beutier T, Boscher D, France M (1995) Salammbo: a three-dimensional simulation of the proton radiation belt. J Geophys Res 100:17181–17188. doi:10.1029/94JA02728

Bortnik J, Thorne RM (2010) Transit time scattering of energetic electrons due to equatorially confined magnetosonic waves. J Geophys Res 115(A07):213. doi:10.1029/2010JA015283

Bortnik J, Thorne RM, Inan US (2008a) Nonlinear interaction of energetic electrons with large amplitude chorus. Geophys Res Lett 35(L21):102. doi:10.1029/2008GL035500

Bortnik J, Thorne RM, Meredith NP (2008b) The unexpected origin of plasmaspheric hiss from discrete chorus emissions. Nature 452:62–66. doi:10.1038/nature06741

Bortnik J, Li W, Thorne RM, Angelopoulos V, Cully C, Bonnell J, Le Contel O, Roux A (2009) An observation linking the origin of plasmaspheric hiss to discrete chorus emissions. Science 324:775. doi:10.1126/science.1171273

Bourdarie S, Boscher D, Beutier T, Sauvaud J, Blanc M (1997) Electron and proton radiation belt dynamic simulations during storm periods: a new asymmetric convection-diffusion model. J Geophys Res 102:17541–17552. doi:10.1029/97JA01305

Burtis WJ, Helliwell RA (1975) Magnetospheric chorus—amplitude and growth rate. J Geophys Res 80:3265–3270. doi:10.1029/JA080i022p03265

Cattell C, Wygant JR, Goetz K, Kersten K, Kellogg PJ, von Rosenvinge T, Bale SD, Roth I, Temerin M, Hudson MK, Mewaldt RA, Wiedenbeck M, Maksimovic M, Ergun R, Acuna M, Russell CT (2008) Discovery of very large amplitude whistler-mode waves in Earth's radiation belts. Geophys Res Lett 35(L01):105. doi:10.1029/2007GL032009

Cully CM, Bonnell JW, Ergun RE (2008) THEMIS observations of long-lived regions of large-amplitude whistler waves in the inner magnetosphere. Geophys Res Lett 35:L17S16, doi:10.1029/2008GL033643

Fok MC, Glocer A, Zheng Q, Horne RB, Meredith NP, Albert JM, Nagai T (2010) Recent developments in the radiation belt environment model. J Atmos Sol Terr Phys. 73:1435–1443. doi:10.1016/j.jastp.2010.09.033

Fraser BJ, Singer HJ, Hughes WJ, Wygant JR, Anderson RR, Hu YD (1996) Crres poynting vector observations of electromagnetic ion cyclotron waves near the plasmapause. J Geophys Res 101:15331–15344. doi:10.1029/95JA03480

Glauert SA, Horne RB (2005) Calculation of pitch angle and energy diffusion coefficients with the PADIE code. J Geophys Res 110(A04):206. doi:10.1029/2004JA010851

Horne RB, Thorne RM (1998) Potential waves for relativistic electron scattering and stochastic acceleration during magnetic storms. Geophys Res Lett 25:3011–3014. doi:10.1029/98GL01002
Horne RB, Thorne RM (2003) Relativistic electron acceleration and precipitation during resonant interactions with whistler-mode chorus. Geophys Res Lett 30:1527. doi:10.1029/2003GL016973
Horne RB, Glauert SA, Thorne RM (2003a) Resonant diffusion of radiation belt electrons by whistler-mode chorus. Geophys Res Lett 30:1493. doi:10.1029/2003GL016963
Horne RB, Meredith NP, Thorne RM, Heynderickx D, Iles RHA, Anderson RR (2003b) Evolution of energetic electron pitch angle distributions during storm time electron acceleration to megaelectronvolt energies. J Geophys Res 108:1016. doi:10.1029/2001JA009165
Horne RB, Thorne RM, Glauert SA, Albert JM, Meredith NP, Anderson RR (2005) Timescale for radiation belt electron acceleration by whistler mode chorus waves. J Geophys Res 110(A03):225. doi:10.1029/2004JA010811
Kennel CF, Engelmann F (1966) Velocity space diffusion from weak plasma turbulence in a magnetic field. Phys Fluids 9:2377–2388. doi:10.1063/1.1761629
Kim J, Ryu D, Jones TW, Hong SS (1999) A multidimensional code for isothermal magnetohydrodynamic flows in astrophysics. Astrophys J 514:506–519. doi:10.1086/306915
Koons HC, Roeder JL (1990) A survey of equatorial magnetospheric wave activity between 5 and 8 R_E. Planet Space Sci 38:1335–1341. doi:10.1016/0032-0633(90)90136-E
Kozyra JU, Rasmussen CE, Miller RH, Lyons LR (1994) Interaction of ring current and radiation belt protons with ducted plasmaspheric hiss. 1: diffusion coefficients and timescales. J Geophys Res 99:4069–4084. doi:10.1029/93JA01532
Li L, Cao J, Zhou G (2005) Combined acceleration of electrons by whistler-mode and compressional ULF turbulences near the geosynchronous orbit. J Geophys Res 110(A03):203. doi:10.1029/2004JA010628
Li W, Shprits YY, Thorne RM (2007) Dynamic evolution of energetic outer zone electrons due to wave-particle interactions during storms. J Geophys Res 112(A11):A10,220, doi:10.1029/2007JA012368
Lyons LR (1974a) Electron diffusion driven by magnetospheric electrostatic waves. J Geophys Res 79:575–580. doi:10.1029/JA079i004p00575
Lyons LR (1974b) General relations for resonant particle diffusion in pitch angle and energy. J Plasma Phys 12:45. doi:10.1017/S0022377800024910
Lyons LR (1974c) Pitch angle and energy diffusion coefficients from resonant interactions with ion-cyclotron and whistler waves. J Plasma Phys 12:417–432
Lyons LR, Thorne RM (1973) Equilibrium structure of radiation belt electrons. J Geophys Res 78:2142–2149. doi:10.1029/JA078i013p02142
Lyons LR, Williams DJ (1984) Quantitative aspects of magnetospheric physics. Springer, New York
Maksimovic M, Pierrard V, Lemaire JF (1997a) A kinetic model of the solar wind with Kappa distribution functions in the corona. Astron Astrophys 324:725–734
Maksimovic M, Pierrard V, Riley P (1997b) Ulysses electron distributions fitted with Kappa functions. Geophys Res Lett 24:1151–1154. doi:10.1029/97GL00992
Meredith NP, Horne RB, Anderson RR (2001) Substorm dependence of chorus amplitudes: implications for the acceleration of electrons to relativistic energies. J Geophys Res 106:13165–13178. doi:10.1029/2000JA900156
Meredith NP, Horne RB, Iles RHA, Thorne RM, Heynderickx D, Anderson RR (2002) Outer zone relativistic electron acceleration associated with substorm-enhanced whistler mode chorus. J Geophys Res 107:1144. doi:10.1029/2001JA900146
Meredith NP, Horne RB, Thorne RM, Anderson RR (2003) Favored regions for chorus-driven electron acceleration to relativistic energies in the earth's outer radiation belt. Geophys Res Lett 30:1871. doi:10.1029/2003GL017698
Meredith NP, Horne RB, Thorne RM, Summers D, Anderson RR (2004) Substorm dependence of plasmaspheric hiss. J Geophys Res 109(A06):209. doi:10.1029/2004JA010387

Meredith NP, Horne RB, Glauert SA, Anderson RR (2007) Slot region electron loss timescales due to plasmaspheric hiss and lightning-generated whistlers. J Geophys Res 112:8214. doi:10.1029/2007JA012413

Nunn D (1974) A self-consistent theory of triggered VLF emissions. Planet Space Sci 22:349–378. doi:10.1016/0032-0633(74)90070-1

O'Brien TP, Lorentzen KR, Mann IR, Meredith NP, Blake JB, Fennell JF, Looper MD, Milling DK, Anderson RR (2003) Energization of relativistic electrons in the presence of ULF power and MeV microbursts: evidence for dual ULF and VLF acceleration. J Geophys Res 108:1329. doi:10.1029/2002JA009784

Orlova KG, Shprits YY (2010) Dependence of pitch-angle scattering rates and loss timescales on the magnetic field model. Geophys Res Lett 370(L05):105. doi:10.1029/2009GL041639

Parrot M, Gaye CA (1994) A statistical survey of ELF waves in a geostationary orbit. Geophys Res Lett 21:2463–2466. doi:10.1029/94GL01700

Roth I, Temerin M, Hudson MK (1999) Resonant enhancement of relativistic electron fluxes during geomagnetically active periods. Ann Geophys 17:631–638. doi:10.1007/s00585-999-0631-2

Russell CT, Holzer RE, Smith EJ (1969) OGO 3 observations of ELF noise in the magnetosphere. 1. Spatial extent and frequency of occurrence. J Geophys Res 74:755–777. doi:10.1029/JA074i003p00755

Santolík O, Gurnett DA, Pickett JS, Parrot M, Cornilleau-Wehrlin N (2003) Spatio-temporal structure of storm-time chorus. J Geophys Res 108:1278. doi:10.1029/2002JA009791

Santolík O, Gurnett DA, Pickett JS, Parrot M, Cornilleau-Wehrlin N (2004) A microscopic and nanoscopic view of storm-time chorus on 31 March 2001. Geophys Res Lett 31(L02):801. doi:10.1029/2003GL018757

Schulz M, Lanzerotti LJ (1974) Particle diffusion in the radiation belts, in physics and chemistry in space, vol 7. Springer, New York

Shprits YY, Thorne RM, Horne RB, Glauert SA, Cartwright M, Russell CT, Baker DN, Kanekal SG (2006) Acceleration mechanism responsible for the formation of the new radiation belt during the 2003 halloween solar storm. Geophys Res Lett 33(L05):104. doi:10.1029/2005GL024256

Shprits YY, Elkington SR, Meredith NP, Subbotin DA (2008) Review of modeling of losses and sources of relativistic electrons in the outer radiation belt I: radial transport. J Atmos Sol Terr Phys 70:1679–1693. doi:10.1016/j.jastp.2008.06.008

Shprits YY, Subbotin DA, Meredith NP, Elkington SR (2008) Review of modeling of losses and sources of relativistic electrons in the outer radiation belt II: local acceleration and loss. J Atmos Sol Terr Phys 70:1694–1713. doi:10.1016/j.jastp.2008.06.014

Shprits YY, Chen L, Thorne RM (2009a) Simulations of pitch angle scattering of relativistic electrons with MLT-dependent diffusion coefficients. J Geophys Res 114(A03):219. doi:10.1029/2008JA013695

Shprits YY, Subbotin D, Ni B (2009b) Evolution of electron fluxes in the outer radiation belt computed with the VERB code. J Geophys Res 114(A11):209. doi:10.1029/2008JA013784

Smith EJ, Frandsen AMA, Tsurutani BT, Thorne RM, Chan KW (1974) Plasmaspheric hiss intensity variations during magnetic storms. J Geophys Res 79:2507–2510. doi:10.1029/JA079i016p02507

Stix TH (1992) Waves in plasmas. American Institute of Physics, New York

Strang G (1968) On the construction and comparison of difference schemes. SIAM J Numer Anal 5:506

Su Z, Zheng H (2008) Simulation of resonant interaction between energetic electrons and whistler-mode chorus in the outer radiation belt. Chin Phys Lett 25:4493–4496

Su Z, Zheng H (2009) Resonant scattering of relativistic outer zone electrons by plasmaspheric plume electromagnetic ion cyclotron waves. Chin Phys Lett 26(129):401. doi:10.1088/0256-307X/26/12/129401

Su Z, Zheng H, Wang S (2009a) Dynamic evolution of energetic outer zone electrons due to whistler-mode chorus based on a realistic density model. J Geophys Res 114(A07):201. doi:10.1029/2008JA014013

Su Z, Zheng H, Wang S (2009b) Evolution of electron pitch angle distribution due to interactions with whistler-mode chorus following substorm injections. J Geophys Res 114(A08):202. doi:10.1029/2009JA014269

Su Z, Zheng H, Xiong M (2009c) Dynamic evolution of outer radiation belt electrons due to whistler-mode chorus. Chin Phys Lett 26(039):401

Su Z, Xiao F, Zheng H, Wang S (2010a) STEERB: a three-dimensional code for storm-time evolution of electron radiation belt. J Geophys Res 115(A09):208. doi:10.1029/2009JA015210

Su Z, Zheng H, Wang S (2010b) A parametric study on the diffuse auroral precipitation by resonant interaction with whistler-mode chorus. J Geophys Res 115(A05):219. doi:10.1029/2009JA014759

Su Z, Zheng H, Wang S (2010c) Three dimensional simulations of energetic outer zone electron dynamics due to wave-particle interaction and azimuthal advection. J Geophys Res 115(A06):203. doi:10.1029/2009JA014980

Su Z, Xiao F, Zheng H, Wang S (2011a) CRRES observation and STEERB simulation of the 9 October 1990 electron radiation belt dropout event. Geophys Res Lett 38(L06):106. doi:10.1029/2011GL046873

Su Z, Xiao F, Zheng H, Wang S (2011b) Radiation belt electron dynamics driven by adiabatic transport, radial diffusion, and wave-particle interactions. J Geophys Res 116(A04):205. doi:10.1029/2010JA016228

Su Z, Zheng H, Chen L, Wang S (2011c) Numerical simulations of storm-time outer radiation belt dynamics by wave-particle interactions including cross diffusion. J Atmos Sol Terr Phys 73:95–105. doi:10.1016/j.jastp.2009.08.002

Subbotin D, Shprits Y, Ni B (2010) Three-dimensional VERB radiation belt simulations including mixed diffusion. J Geophys Res 115(A03):205. doi:10.1029/2009JA015070

Summers D (2005) Quasi-linear diffusion coefficients for field-aligned electromagnetic waves with applications to the magnetosphere. J Geophys Res 110(A08):213. doi:10.1029/2005JA011159

Summers D, Ma C (2000) A model for generating relativistic electrons in the Earth's inner magnetosphere based on gyroresonant wave-particle interactions. J Geophys Res 105:2625

Summers D, Omura Y (2007) Ultra-relativistic acceleration of electrons in planetary magnetospheres. Geophys Res Lett 34(L24):205. doi:10.1029/2007GL032226

Summers D, Thorne RM (2003) Relativistic electron pitch-angle scattering by electromagnetic ion cyclotron waves during geomagnetic storms. J Geophys Res 108:1143. doi:10.1029/2002JA009489

Summers D, Thorne RM, Xiao F (1998) Relativistic theory of wave-particle resonant diffusion with application to electron acceleration in the magnetosphere. J Geophys Res 103(20):487

Summers D, Ni B, Meredith NP (2007a) Timescales for radiation belt electron acceleration and loss due to resonant wave-particle interactions: 1. Theor J Geophys Res 112(A04):206. doi:10.1029/2006JA011801

Summers D, Ni B, Meredith NP (2007b) Timescales for radiation belt electron acceleration and loss due to resonant wave-particle interactions: 2. Evaluation for VLF chorus, ELF hiss, and electromagnetic ion cyclotron waves. J Geophys Res 112(A04):207. doi:10.1029/2006JA011993

Summers D, Ni B, Meredith NP, Horne RB, Thorne RM, Moldwin MB, Anderson RR (2008) Electron scattering by whistler-mode elf hiss in plasmaspheric plumes. J Geophys Res 113(A04):219. doi:10.1029/2007JA012678

Tao X, Chan AA, Albert JM, Miller JA (2008) Stochastic modeling of multidimensional diffusion in the radiation belts. J Geophys Res 113(A07):212. doi:10.1029/2007JA012985

Tao X, Albert JM, Chan AA (2009) Numerical modeling of multidimensional diffusion in the radiation belts using layer methods. J Geophys Res 114(A02):215. doi:10.1029/2008JA013826

Tao X, Bortnik J, Albert JM, Liu K, Thorne RM (2011a) Comparison of quasilinear diffusion coefficients for parallel propagating whistler mode waves with test particle simulations. Geophys Res Lett 380(L06):105. doi:10.1029/2011GL046787

Tao X, Thorne RM, Li W, Ni B, Meredith NP, Horne RB (2011b) Evolution of electron pitch angle distributions following injection from the plasma sheet. J Geophys Res 116(A4): A04,229

Thorne RM (2010) Radiation belt dynamics: the importance of wave-particle interactions. Geophys Res Lett 37(L22):107. doi:10.1029/2010GL044990

Thorne RM, Smith EJ, Burton RK, Holzer RE (1973) Plasmaspheric hiss. J Geophys Res 78: 1581–1596. doi:10.1029/JA078i010p01581

Thorne RM, Ni B, Tao X, Horne RB, Meredith NP (2010) Scattering by chorus waves as the dominant cause of diffuse auroral precipitation. Nature 467:943. doi:10.1038/nature09467

Tsurutani BT, Smith EJ (1974) Postmidnight chorus: a substorm phenomenon. J Geophys Res 79:118–127. doi:10.1029/JA079i001p00118

Tsurutani BT, Smith EJ (1977) Two types of magnetospheric ELF chorus and their substorm dependences. J Geophys Res 82:5112–5128. doi:10.1029/JA082i032p05112

Varotsou A, Boscher D, Bourdarie S, Horne RB, Glauert SA, Meredith NP (2005) Simulation of the outer radiation belt electrons near geosynchronous orbit including both radial diffusion and resonant interaction with whistler-mode chorus waves. Geophys Res Lett 32(L19):106. doi: 10.1029/2005GL023282

Varotsou A, Boscher D, Bourdarie S, Horne RB, Meredith NP, Glauert SA, Friedel RH (2008) Three-dimensional test simulations of the outer radiation belt electron dynamics including electron-chorus resonant interactions. J Geophys Res 113(A12):212. doi:10.1029/2007JA012862

Vasyliunas VM (1968) A survey of low-energy electrons in the evening sector of the magnetosphere with OGO 1 and OGO 3. J Geophys Res 73:2839

Viñas AF, Mace RL, Benson RF (2005) Dispersion characteristics for plasma resonances of Maxwellian and Kappa distribution plasmas and their comparisons to the IMAGE/RPI observations. J Geophys Res 110(A06):202. doi:10.1029/2004JA010967

Xiao F (2006) Modelling energetic particles by a relativistic kappa loss cone distribution function in plasmas. Plasma Phys Controlled Fusion 48:203

Xiao F, He HY (2006) Energetic electron pitch angle diffusion due to whistler wave during terrestrial storms. Chin Phys Lett 23:267–270. doi:10.1088/0256-307X/23/1/077

Xiao F, Chen L, Zhou Q, He H, Wen Y (2007a) Bounce-averaged acceleration of energetic electrons by whistler mode chorus in the magnetosphere. Chin Phys Lett 24:294–297. doi:10.1088/0256-307X/24/1/080

Xiao F, Thorne RM, Summers D (2007b) Higher-order gyroresonant acceleration of electrons by superluminous (AKR) wave-modes. Planet Space Sci 55:1257

Xiao F, Chen L, Li J (2008a) Energetic particles modeled by a generalized relativistic kappa-type distribution function in plasmas. Plasma Phys Controlled Fusion 50(105):002. doi:10.1088/0741-3335/50/10/105002

Xiao F, Shen C, Wang Y, Zheng H, Wang S (2008b) Energetic electron distributions fitted with a relativistic kappa-type function at geosynchronous orbit. J Geophys Res 113(A05):203. doi: 10.1029/2007JA012903

Xiao F, Zhou Q, Li C, Cai A (2008c) Modeling solar energetic particle by a relativistic kappa-type distribution. Plasma Phys Controlled Fusion 50(062):001. doi:10.1088/0741-3335/50/6/062001

Xiao F, Su Z, Zheng H, Wang S (2009) Modeling of outer radiation belt electrons by multidimensional diffusion process. J Geophys Res 114(A03):201. doi:10.1029/2008JA013580

Xiao F, Chen L, Su Z, Zheng H, Wang S (2010a) A parametric study on outer radiation belt electron evolution by superluminous R-X mode waves. J Geophys Res 115(A10):217. doi: 10.1029/2010JA015374

Xiao F, Su Z, Zheng H, Wang S (2010b) Three-dimensional simulations of outer radiation belt electron dynamics including cross diffusion terms. J Geophys Res 115(A05):216. doi:10.1029/2009JA014541

Xiao F, Chen L, He Y, Su Z, Zheng H (2011) Modeling of precipitation loss of ring current protons by electromagnetic ion cyclotron waves. J Atmos Sol Terr Phys 73:106–111. doi:10.1016/j.jastp.2010.01.007

Yoon PH (2011) Large-amplitude whistler waves and electron acceleration. Geophys Res Lett 381(L12):105. doi:10.1029/2011GL047893

Zheng H, Su Z, Xiong M (2008) Pitch angle distribution evolution of energetic electrons by whistler-mode chorus. Chin Phys Lett 25:3515–3518. doi:10.1088/0256-307X/25/9/113

Zheng Q, Fok M, Albert J, Horne RB, Meredith NP (2011) Effects of energy and pitch angle mixed diffusion on radiation belt electrons. J Atmos Sol Terr Phys 73:785–795. doi:10.1016/j.jastp.2011.01.014

http://www.springer.com/978-3-662-46650-6

A Global Kinetic Model for Electron Radiation Belt Formation and Evolution

Su, Z.

2015, XI, 106 p. 46 illus., 39 illus. in color., Hardcover
ISBN: 978-3-662-46650-6